Biochimica et Biophysica Acta, 546 (1979) 394—417

BBA 47667

SPECTROSCOPIC AND KINETIC PROPERTIES OF THE TRANSIENT INTERMEDIATE ACCEPTOR IN REACTION CENTERS OF *RHODOPSEUDOMONAS SPHAEROIDES*

M.Y. OKAMURA, R.A. ISAACSON and G. FEHER

University of California San Diego, La Jolla, CA 92093 (U.S.A.)

(Received October 23rd, 1978)

Key words: Reaction center; Transient intermediate acceptor; (Spectroscopy, Kinetics, Rhodopseudomonas sphaeroides)

Summary

The photoreductive trapping of the transient, intermediate acceptor, I^-, in purified reaction centers of *Rhodopseudomonas sphaeroides* R-26 was investigated for different external conditions. The optical spectrum of I^- was found to be similar to that reported for other systems by Shuvalov and Klimov ((1976) Biochim. Biophys. Acta 440, 587—599) and Tiede et al. (P.M. Tiede, R.C. Prince, G.H. Reed and P.L. Dutton (1976) FEBS Lett. 65, 301—304). The optical changes of I^- showed characteristics of both bacteriopheophytin (e.g. bleaching at 762, 542 nm and red shift at 400 nm) and bacteriochlorophyll (bleaching at 802 and 590 nm). Two types of EPR signals of I^- were observed: one was a narrow singlet at $g = 2.0035$, $\Delta H = 13.5$ G, the other a doublet with a splitting of 60 G centered around $g = 2.00$, which was only seen after short illumination times in reaction centers reconstituted with menaquinone. The optical and EPR kinetics of I^- on illumination in the presence of reduced cytochrome *c* and dithionite strongly support the following three-step scheme in which the doublet EPR signal is due to the unstable state $DI^-Q^-Fe^{2+}$ and the singlet EPR signal is due to $DI^-Q^{2-}Fe^{2+}$.

$$DI(Q^-Fe^{2+}) \xrightarrow[k_1 = 1/\tau_1]{cyt^{2+} \overset{h\nu}{\rightarrow} cyt^{3+}} DI^-(Q^-Fe^{2+}) \xrightarrow[k_2 = 1/\tau_2]{\text{dark reaction}} DI(Q^{2-}Fe^{2+}) \underset{k_4 = 1/\tau_4}{\overset{cyt^{2+} \overset{h\nu}{\rightarrow} cyt^{3+}}{\underset{\leftarrow}{\rightarrow}}} DI^-(Q^{2-}Fe^{2+}).$$

where D is the primary donor $(BChl)_2^+$.

Abbreviations: A, primary acceptor; D, primary donor; I, intermediate acceptor; RC, reaction center; Q, quinone; UQ, ubiquinone; MQ, menaquinone; LDAO, lauryldimethylamine oxide; EPR, electron paramagnetic resonance.

The above model was supported by the following observations:

(1) During the first illumination, sigmoidal kinetics of the formation of I^- was observed. This is a direct consequence of the three-sequential reactions.

(2) During the second and subsequent illuminations first-order (exponential) kinetics were observed for the formation of I^-. This is due to the dark decay, k_4, to the state $DIQ^{2-}Fe^{2+}$ formed after the first illumination.

(3) Removal of the quinone resulted in first-order kinetics. In this case, only the first step, k_1, is operative.

(4) The observation of the doublet signal in reaction centers containing menaquinone but not ubiquinone is explained by the longer lifetime of the doublet species $I^-(Q^-Fe^{2+})$ in reaction centers containing menaquinone. The value of τ_2 was determined from kinetic measurements to be 0.01 s for ubiquinone and 4 s for menaquinone ($T = 20°C$).

The temperature and pH dependence of the dark electron transfer reaction $I^-(Q^-Fe^{2+}) \rightarrow I(Q^{2-}Fe^{2+})$ was studied in detail. The activation energy for this process was found to be 0.42 eV for reaction centers containing ubiquinone and 0.67 eV for reaction centers with menaquinone. The activation energy and the doublet splitting were used to calculate the rate of electron transfer from I^- to MQ^-Fe^{2+} using Hopfield's theory for thermally activated electron tunneling. The calculated rate agrees well with the experimentally determined rate which provides support for electron tunneling as the mechanism for electron transfer in this reaction. Using the EPR doublet splitting and the activation energy for electron transfer, the tunneling matrix element was calculated to be 10^{-3} eV. From this value the distance between I^- and MQ^- was estimated to be 7.5—10 Å.

Introduction

The primary process in bacterial photosynthesis takes place in a membrane bound bacteriochlorophyll-protein called the reaction center and involves the photochemical electron transfer from the primary electron donor D (a bacteriochlorophyll dimer) to the primary electron acceptor Q Fe^{2+} (a quinone-iron (ferroquinone) complex) resulting in a charge separation stabilized for times of the order of milliseconds [1,2]. Recent evidence has indicated the involvement at shorter times of a transient, intermediate acceptor species I, which accepts the electron from the bacteriochlorophyll dimer and passes it on to the quinone-iron acceptor. The evidence for this intermediate acceptor comes from the observation of a short lived transient state (P^f), first observed by Parson et al., when the quinone-iron acceptor was reduced [3]. This state was shown by picosecond spectroscopy [4,5] to be in the primary photochemical pathway of reaction centers in which the quinone-iron acceptor was not reduced. This intermediate state, P^f, exhibits spectroscopic changes at 1250 nm [6,7] that are associated with the oxidation of the primary donor D. Thus, P^f was identified as an oxidized donor-reduced acceptor pair [6,7]. Since the presence of the quinone-iron acceptor was not necessary for the formation of P^f, an additional, intermediate acceptor must be present, i.e. $P^f = D^+I^-$. On the basis of optical spectral studies of model compounds, Fajer et al. proposed that this inter-

mediate acceptor I is bacteriopheophytin [8]. Further characterization of I was hampered by the short lifetime of the P^+I^- state ($t_{1/2}$ = 10 ns) [9].

Recently, several groups of investigators have reported the trapping of I^- in subchromatophore preparations from *Chromatium minutismum* [10], *Thiocapsa reseopersicina* [10], *Chromatium vinosum* [11—14], and *Rhodopseudomonas viridis* [15—19] illuminated at a low redox potential. These preparations contain a tightly bound fast (of the order of microseconds) reacting cytochrome which can transfer an electron to the oxidized donor, thereby trapping I^- by preventing the recombination of the electron on I^- with the positive charge on D^+, i.e.:

$$DI(Q^-Fe^{2+}) \overset{h\nu}{\rightleftharpoons} D^+I^-(Q^-Fe^{2+}) \xrightarrow{cyt^{2+}\ cyt^{3+}} DI^-(Q^-Fe^{2+}). \quad (1)$$

Of particular interest was the observation by Tiede et al. of an EPR spectrum consisting of a narrow EPR signal flanked by two additional lines (doublet) [11]. The doublet structure was postulated to arise from an interaction between I^- and the reduced acceptor Q^-Fe^{2+} and thus harbors information about the distance and electron transfer rate between these two species.

Since the reaction center of *Rps. sphaeroides* R-26 is the most completely characterized photosynthetic unit, it was of interest to trap and investigate I^- in that system. Although this preparation contains no cytochrome *c*, initial experiments [19] showed that by illuminating reaction centers in the presence of exogenous cytochrome *c* and dithionite, changes in optical spectra characteristic of I^- were obtained. However, the doublet EPR signal was not present in these samples and only a single narrow EPR line was observed. In addition, a lag in the formation of I was observed during the first illumination of the sample. This lag disappeared during subsequent illuminations. In order to explain these findings, the following three-step model was postulated for the formation of I^- * in *Rps. sphaeroides* reaction centers [19]:

$$\begin{array}{lcccccc} \text{Broad EPR} & & & & & & \text{Narrow EPR} \\ g = 1.83 & & \text{Doublet EPR} & & \text{No EPR} & & g = 2.0036 \\ \downarrow & & \downarrow & & \downarrow & & \downarrow \\ DI(Q^-Fe^{2+}) & \xrightarrow[k_1 = 1/\tau_1]{cyt^{2+}\ h\nu\ cyt^{3+}} & DI^-(Q^-Fe^{2+}) & \xrightarrow[k_2 = 1/\tau_2]{\text{dark reaction}} & DI(Q^{2-}Fe^{2+}) & \underset{k_4 = 1/\tau_4}{\overset{cyt^{2+}\ h\nu\ cyt^{3+}}{\rightleftharpoons}}\ {\scriptstyle k_3 = 1/\tau_3} & DI^-(Q^{2-}Fe^{2+}) \end{array} \quad (2)$$

where k_1 (and similarly, k_3) involve a two-step trapping process as shown in Eqn. 1.

The work described in this paper was undertaken to test the three-step model quantitatively, to determine the rate constants, to understand the origin of the doublet EPR spectrum, and to find out why no doublet structure was observed in reaction centers from *Rps. sphaeroides*. The ultimate goal is to understand the nature of I and the interactions with its environment.

Materials and Methods

Reaction centers were prepared by treatment with the detergent LDAO (Onyx Chemical Co.) as described earlier [1]. Since reducing agents are known

* The secondary ubiquinone that is present in reaction centers is assumed to remain fully reduced (i.e. diamagnetic) in the presence of dithionite and for the sake of simplicity has been omitted from Eqn. 2.

to react with LDAO, this detergent was replaced by Triton X-100 (Sigma Chemical Co.) by washing reaction centers bound to a DEAE-cellulose (Whatman DE52) column with 0.1% Triton X-100, followed by elution with 1 M NaCl and dialysis in buffers containing 0.1% Triton (10 mM Tris, pH 8). Quinone removal and reconstitution with either UQ-10 (Sigma Chemical Co.) or MQ (vitamin K-1) (Sigma Chemical Co.) were performed as previously described [20]. The concentration of the reaction centers was determined optically by using the molar extinction coefficient $\epsilon^{802} = 2.88 \cdot 10^5\ M^{-1} \cdot cm^{-1}$ [21].

Optical samples were typically prepared in gas-tight sample cells 1-cm path length, stoppered with serum caps and purged with argon. In a typical experiment, 1.5 ml reaction centers (0.1% Triton, 50 mM Tris, pH 8) which contained 0.2 mM cytochrome *c* (horse heart, Sigma, Type III) were deoxygenated by repeated evacuation and argon purge cycles. Then, 15 μl of freshly prepared 0.2 M NaS_2O_4 (in 1 M Tris, pH 8) was added.

Optical measurements were made using a CARY 14R spectrometer. Kinetic measurements were typically made by side illumination using a tungsten projector lamp and Corning filters CS-2-64, CS-5-56, 3 cm water, to admit wavelengths 750 nm $< \lambda <$ 950 nm ($I \approx 0.2\ W/cm^2$, measured with a YSI Radiometer). In some cases, a broad band interference filter centered at 850 nm (Corion No. 50, BB-8500) or unfiltered light was used. Flash kinetics were performed on an instrument described earlier [22]. A camera flash (Norman 2000, $400\ W \cdot s^{-1}$ input energy, $0.3\ J/cm^2$ output energy, 1 ms half duration) and Corning filters CS-2-64 and CS-5-56 were used ($\lambda > 750$ nm). A silicon diode detector, United Detector Technology PIN 10D, protected by interference filters, and a Bausch and Lomb monochromator were used.

The temperature dependence of the rates was determined using a thermostated cell holder. The temperature of the sample was measured using a 44018 YSI Thermilinear network calibrated by comparison with several precision thermometers. pH measurements were obtained at 20°C using a Radiometer PM64 pH meter and a Radiometer GK2401C electrode. The ionic strength of the buffers at different pH values were maintained constant by addition of NaCl.

EPR spectra were obtained at 2.1 K with a 9 GHz superheterodyne spectrometer of local design [23] utilizing 80 Hz field modulation. The spectra are thus first derivative traces. Samples were prepared in argon purged gas-tight EPR cells (3 mm or 8 mm diameter) containing 0.2 mM cytochrome *c*, 2 mM dithionite, 60 mM Tris, pH 8, 0.1% Triton X-100. In some cases, excess quinone was added, dissolved in 10% Triton X-100. The samples were illuminated using a tungsten light source filtered through 3-cm water and Corning Filters CS2-64 and 5-56 (unless otherwise indicated), then quickly frozen in a hexane slurry ($T = -100$°C). In order to freeze samples rapidly without cracking the tubes, a short piece of Teflon tubing which was sealed on the bottom was inserted into the sample tube prior to freezing.

Experimental results and Analyses

Optical spectrum of the trapped intermediate

When reaction centers from *Rps. sphaeroides* were illuminated at room

temperature pH 8 in the presence of exogenous mammalian cytochrome *c* and dithionite, optical spectral changes characteristic of the trapped I^- [10,12,14] were observed (Fig. 1). The changes were produced in 10—20 s ($I \approx 0.2$ W/cm^2) and in the dark decayed slowly ($t_{1/2}$ = 15—20 min). Note that in the presence of excess dithionite, oxidized cytochrome is rapidly re-reduced so that changes due to cytochrome are not observed.

The rate of formation increased linearly with light intensity up to 0.2 W/cm^2. Above this intensity a deviation from linearity, most likely due to a temperature rise of the sample, was observed. The rate of formation was also proportional to cytochrome concentration below 0.2 mM cytochrome. At

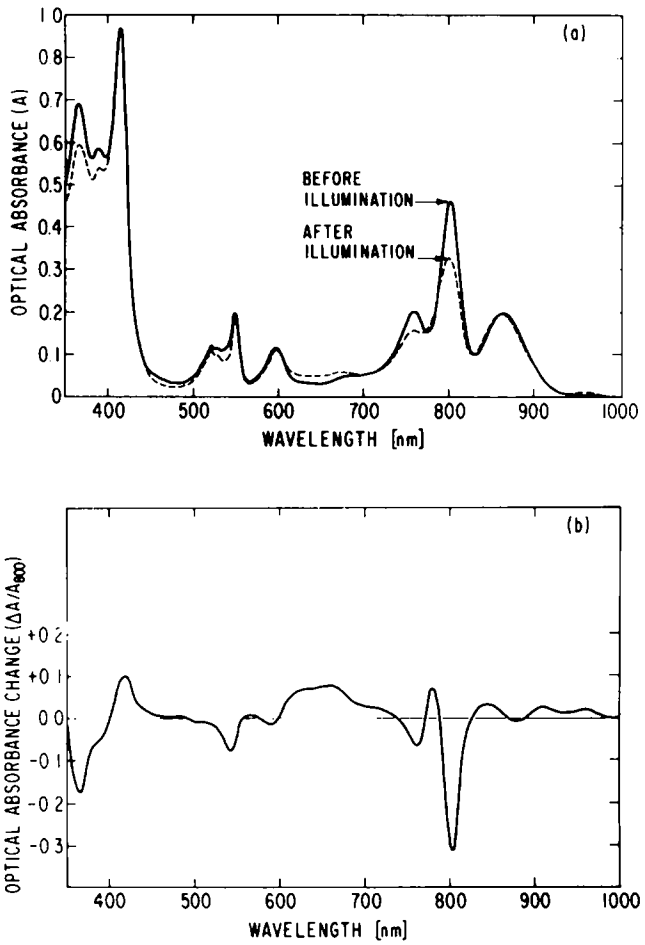

Fig. 1. Changes in the optical absorption spectrum of *R. sphaeroides* reaction centers with actinic illumination ($I \approx 0.2$ W/cm^2, 2 min) in the presence of 0.2 mM cytochrome *c* and 2 mM dithionite (pH 8, T = 25°C). (a) Spectra taken before and after illumination (0.3 mm pathlength) [RC] = 5.5 · 10^{-5} M. (b) Light minus dark difference spectrum obtained with illuminated cell in the sample compartment and dark sample in the reference compartment (for λ = 600—1000 nm, [RC] = 2 · 10^{-5} M, for λ = 350—600 nm, [RC] = 1 · 10^{-5} M, [cyt] = 4 · 10^{-5} M. Absorbance changes normalized to A_{800}. The times required for scanning the spectra (2—3 min) were short compared to the decay of I^- ($t_{1/2}$ = 15—20 min).

higher concentration of cytochrome the rate was independent of concentration indicating saturation of the cytochrome binding sites.

The changes due to the trapped I^- include bleaching at 762 and 542 nm, a hyperchromic (red) shift around 400 nm, characteristic of bacteriopheophytin, and bleaching at 802 and 590 nm, characteristic of BChl. In addition, a broad absorption increase in the 600—700 nm region, as well as increases at 845, 910, and 962 nm were observed. These latter changes are similar but not identical to those seen in $BChl^-$ and $BPhe^-$ [8,24].

The singlet EPR spectrum of the trapped intermediate in reaction centers of Rps. sphaeroides

Illumination of reaction centers at 25°C in the presence of cytochrome *c* and dithionite also resulted in changes in its low temperature (2.1 K) EPR spectrum (see Fig. 2). Before illumination, the EPR spectrum was that of the reduced ferroquinone, A^- ($g = 1.8$); in addition, a small amount (≈5%) of free radical signal ($g = 2.0045$) assigned to a ubisemiquinone was observed (Fig. 2a). After illumination, a narrow signal appeared at $g = 2.0036$, $\Delta H = 13.0$ G, and the ferroquinone signal A^- disappeared (Fig. 2b). The narrow signal consists of a single line (Fig. 3a) and differs from the EPR spectrum seen in *C. vinosum* chromatophores illuminated at 200 K, where an additional doublet spectrum was observed (see Fig. 3b). The absence of the doublet and the disappearance of the $g = 1.8$ signal led to the three-step model in which the doublet due to

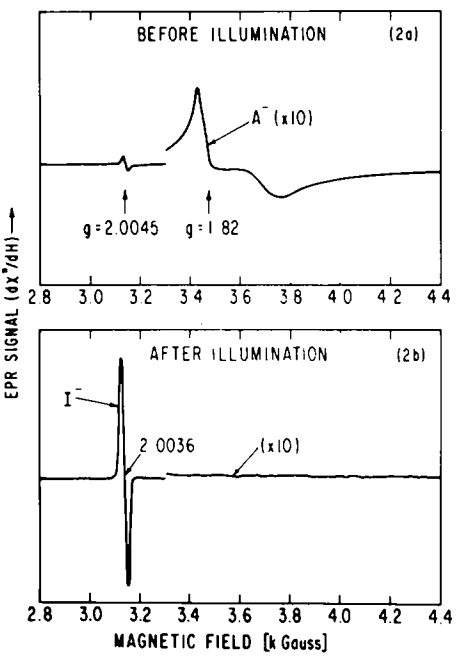

Fig. 2. Changes in the EPR spectrum ($T = 2.1$ K) of *R. sphaeroides* reaction centers after illumination ($I = 0.8$ W/cm^2, 5 min, $T = 25$°C) in the presence of 0.2 mM cytochrome *c* and 2 mM dithionite, pH 8 (vol = 1 ml, 8 mm internal diameter quartz tubes, $\nu = 8.85$ GHz, microwave power ≈10^{-6} W, modulation amplitude = 20 G, [RC] = $6 \cdot 10^{-5}$ M.) (a) Before illumination. (b) After illumination.

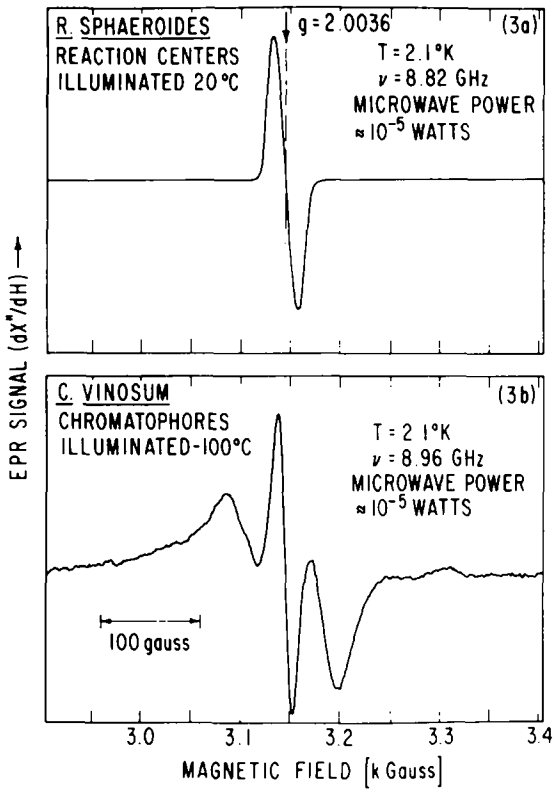

Fig. 3. Comparison between EPR signals (T = 2.1 K) seen in (a) *R. sphaeroides* reaction centers ($6 \cdot 10^{-5}$ M) illuminated at 25°C (0.8 W/cm^2, 5 min) in the presence of 0.2 mM cytochrome *c* (0.1% Triton X-100) and (b) *C. vinosum* chromatophores (A_{800}^{1cm} = 100) illuminated at −100°C (I = 0.8 W/cm^2, 15 min). Both samples contained 2 mM dithionite, 60 mM Tris, pH 8. Sample volumes 1 ml. Modulation amplitude = 10 G.

I^-Q^- decays in the dark to IQ^{2-} and the narrow, singlet signal is due to I^-Q^{2-} (see Introduction).

The doublet EPR signal of the trapped intermediate in reaction centers of Rps. sphaeroides

In order to try to observe the doublet EPR signal in reaction centers of *Rps. sphaeroides*, several modifications in the experimental procedure were introduced to try to simulate the conditions under which the doublet was produced in chromatophores of *C. vinosum*. One of these was the low (−100°C) temperature at which I^- was formed in *C. vinosum*. Reaction centers from *Rps. sphaeroides* do not contain a tightly bound cytochrome capable of rapidly reducing D^+ at subzero temperatures, as do chromatophores of *C. vinosum*. Consequently, low temperature illumination of reaction centers from *Rps. sphaeroides* cannot generate I^-. However, attempts were made to form I^- at room temperature and to freeze the sample rapidly (≈2 s) while illuminating it (I = 2 W/cm^2). These were the conditions under which Evans et al. observed the first doublet EPR signals in chromatophores from *C. vinosum* [25]. The low

temperature EPR spectra of reaction centers from *Rps. sphaeroides* that were treated this way, however, showed no signs of a doublet.

Another difference between reaction centers from *Rps. sphaeroides* and *C. vinosum* is the nature of their primary quinone: *Rps. sphaeroides* has a ubiquinone (UQ), whereas *C. vinosum* has a menaquinone (MQ) [26,27]. Consequently, experiments were performed on reaction centers of *Rps. sphaeroides* from which UQ had been removed and replaced by MQ (vitamin K-1). Such a reconstituted sample when rapidly frozen after short intense illumination (I = 2 W/cm^2, t = 2 s, T = 8°C) did give a doublet EPR signal (Fig. 4a, b). At low microwave power (Fig. 4a), a singlet EPR signal was also observed which is partly due to the g = 2.0045 dark signal (similar to Fig. 2a) and partly due to a new resonance. At high microwave power (Fig. 4b), the singlet saturates and the EPR spectrum of the doublet predominates. The doublet splitting δH was equal to 60 G (Fig. 4b), similar to that observed in *C. vinosum* [11—13]. When the reaction center sample containing MQ was illuminated for a long period (t = 120 s) prior to freezing, the EPR spectrum of the doublet disappeared and was replaced by a narrow resonance (g = 2.0036, ΔH = 13 G) (Fig. 4c, d), similar to that observed in reaction centers containing UQ (Fig. 3b).

Why is the doublet seen in reaction centers containing MQ but not in those containing UQ? One possibility is that I^-UQ^- does not give a doublet spectrum.

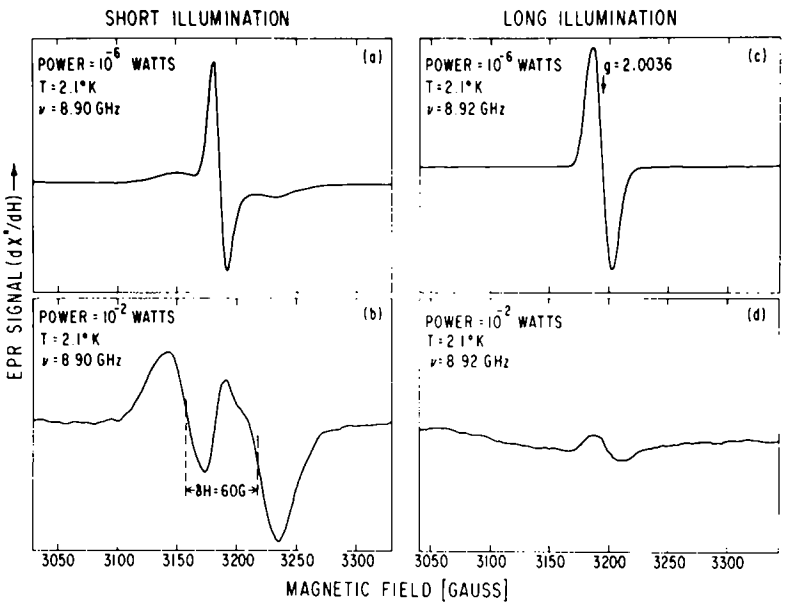

Fig. 4. EPR spectra of reaction centers reconstituted with MQ (vitamin K-1) after short (a and b) and long (c and d) illumination. Reaction centers ($2 \cdot 10^{-5}$ M) were depleted of UQ [19], then reconstituted with MQ (vitamin K-1, 10^{-4} M) in 0.2% Triton X-100, 60 mM Tris-Cl, 2 mM dithionite, 0.2 mM cytochrome c, 1 ml volume. (a) Reaction center sample quickly frozen in hexane slurry (T = —100°C) after short, 2-s illumination at T = 5°C, I = 3 W/cm^2, tungsten lamp, water filter. Microwave power = 10^{-6} W. (b) Same as (a), except microwave power = 10^{-2} W. (c) Reaction center sample frozen after long illumination (2 min at I = 0.2 W/cm^2, tungsten lamp, water filter, microwave power = 10^{-6} W). (d) Same as (c), except microwave power = 10^{-2} W. Spectrometer gain used to obtain spectrum 4a was six times that for 4c. Gains for 4b and 4d were equal. Modulation amplitude 10 G for all spectra.

This would be the case if, for instance, the magnetic interaction between I^- and UQ^-Fe^{2+} was too weak. Another possibility is that I^-UQ^- decays too rapidly to be trapped by rapid freezing. In order to differentiate between these two possibilities, the kinetics of I^- formation were studied.

Kinetics of I^- formation from optical absorbance changes

Reaction centers containing ubiquinone. The optical absorbance changes at 645 nm due to the formation of I^- (Fig. 1b) showed an unusual sigmoidal behavior after the first illumination (Fig. 5a). These changes were slowly reversible in the dark, with a decay half time $t_{1/2}$ = 15—20 min. This decay rate, k_4, is nonexponential and variable. The mechanism of this back reaction (i.e. what is oxidizing I^-) is not understood at present.

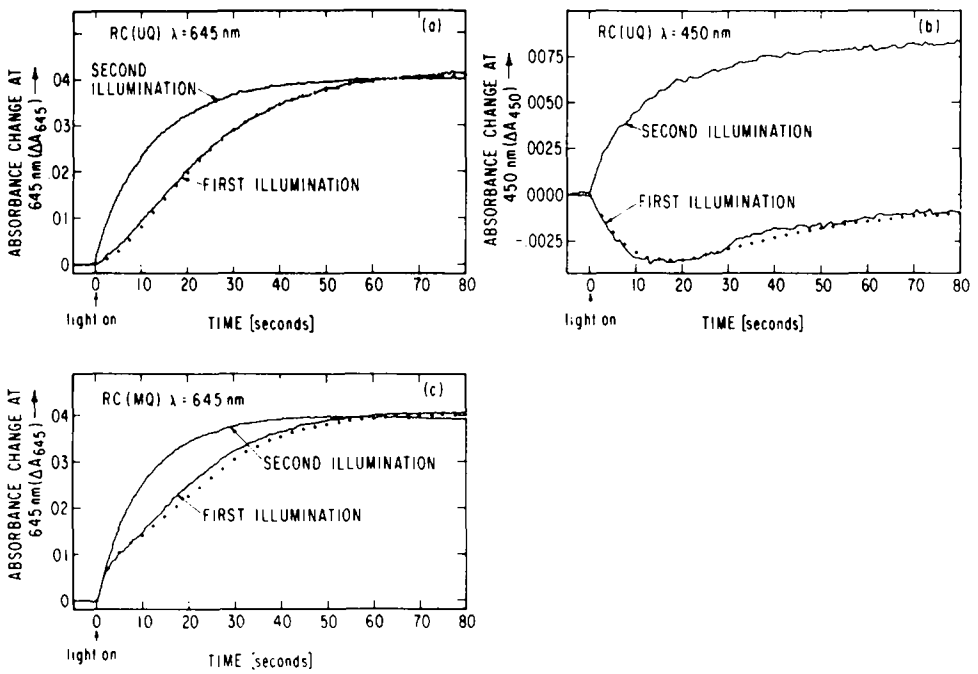

Fig. 5. Kinetics of optical absorbance changes at different wavelengths of reaction centers containing either UQ or MQ. Full lines represent experimental results, dots are theoretical fits. (a) Absorbance changes at λ = 645 nm in reaction centers of *R. sphaeroides* due to formation of I^- (T = 25°C, I = 0.2 W/cm^2) [RC] = 1.9 · 10^{-6} M, [UQ] = 10^{-5} M, 0.2 mM cytochrome *c*, 2 mM dithionite, 60 mM Tris-Cl, pH 8, 0.1% Triton X-100. The second illumination was obtained after a one-hour dark period. The theoretical curve (· · · · · ·) was obtained from Eqns. 18, 11, and 13, using k_2 = 100 s^{-1}, and $k_3 = k_1 = 1/\tau$, where τ = 12.3 s was the exponential time for I^- formation measured during the second illumination. Similar fits could be obtained for any $k_2 > 20$ s^{-1}. (b) Kinetics of optical absorbance changes in reaction centers of *R. sphaeroides* at λ = 450 nm. (Same conditions as in (a).) The theoretical curve (· · · · · ·) was obtained from Eqns. 19, 11, 12, and 13, using k_2 = 100, and $k_3 = k_1 = 1/\tau$, where τ = 15.5 s was the exponential time for I^- formation measured during the second illumination. The molar differential extinction coefficients, $\Delta\epsilon_{da}$, $\Delta\epsilon_{ba}$, $\Delta\epsilon_{ca}$, from Eqns. 14, 16, and 17 were —520, 4300 and —4800 M^{-1} · cm^{-1}, respectively. (c) Kinetics of optical absorbance changes at λ = 645 nm in reaction centers of *R. sphaeroides* containing MQ. Reaction centers reconstituted with MQ were used, otherwise, the conditions were the same as in (a), [MQ] = 10^{-5} M. The theoretical curve (· · · · · ·) was obtained from Eqns. 18, 11, and 13, using k_2 = 0.22 s^{-1}, and $k_3 = k_1 = 1/\tau$, where τ = 10 s was the exponential time for I^- formation during the second illumination.

If the reaction centers were illuminated a second time (after dark recovery), absorbance changes of the same magnitude were observed. However, the kinetics showed exponential rather than sigmoidal behavior (Fig. 5a). Similar exponential kinetics were observed during subsequent illuminations. The sigmoidal behavior was not restored even after a long (≈10 h) dark period. If, however, after the first illumination the sample was oxidized with O_2, re-reduced with dithionite, then illuminated, sigmoidal behavior was again observed. These results are explained by the three-step model, as follows: (1) The sigmoidal shape on the first illumination is a consequence of having three sequential reactions. (2) The exponential behavior on the second illumination can be explained if the last reaction is reversible only back to the state $DI(Q^{2-}Fe^{2+})$. Thus, during the second illumination only one step of the sequence (i.e. k_3 in Eqn. 2) is observed. (3) In the presence of O_2 the reaction centers would be oxidized back to $DI(QFe^{2+})$ so that reduction and illumination could give the three-step reaction sequence under strongly reducing conditions. It is interesting that the primary quinone can be photoreduced to form Q^{2-} but cannot be chemically reduced to Q^{2-} by dithionite in the dark. This is most likely due to kinetic constraints (e.g. inaccessibility of reductant).

The kinetic behavior described above has been quantitatively explained by the three-step model (see Appendix) in which the rate constant k_3 was obtained from the measured rate of formation of I^- during the second illumination. The experimental data were fitted well with the following values: $k_1/k_3 = 1.0$ and k_2/k_3 large ($k_2/k_3 > 20$). The absorbance changes during the first illumination have a characteristic zero initial slope. This is due to the rapid decay of I^-Q^- which prevents the initial formation of I^-. Under these conditions, the kinetics are fairly sensitive to the value of k_1/k_3 (see Appendix, Fig. 10a) but are very insensitive to k_2 whose exact value, therefore, cannot be determined from this experiment (see Appendix, Fig. 10b). Fig. 5a shows a comparison between the experimental data and the theoretical curve (dotted line) with $k_2/k_1 = 100$. Similar theoretical curves are obtained for any $k_2/k_1 > 20$. From this result, using the measured value of $k_3 = k_1 = 0.1\ s^{-1}$, we can estimate an upper limit for the lifetime of I^-UQ^- of $\tau_2 = 1/k_2 < 0.5$ s (a more precise value of τ_2 is given in a later section). This short lifetime is most likely responsible for the lack of a doublet EPR signal in reaction centers containing UQ.

Similar sigmoidal kinetics were also obtained at 800, 760, and 540 nm, where only optical changes due to I^- are observed. However, when the kinetics were measured at 450 nm, where UQ^- also absorbs, different kinetic curves were obtained (Fig. 5b). During the first illumination the absorbance changes were initially negative, then went through a minimum and became again more positive. The absorbance changes on the second illumination were positive and exhibited exponential behavior. This can again be accounted for by the three-step model if the optical absorption changes due to I^- and Q^- have opposite signs. Since k_2 is large, the only initial change is due to the disappearance of Q^-, i.e. the reduction of IQ^- to IQ^{2-} (see Eqn. 2) resulting in an initial decrease in absorption. The subsequent increase in absorbance is due to the subsequent formation of the reduced intermediate acceptor I^-Q^{2-}. These kinetic data were quantitatively fitted with the three-step model using the experimentally determined extinction coefficients connecting the three states, I^-Q^-, IQ^{2-}, and I^-Q^{2-}

(see Appendix). Good agreement between experiment (full line) and theory (dotted line) is obtained as shown in Fig. 5b. The value obtained for the molar differential extinction coefficient for the change from the state IQ^- to IQ^{2-}, $\Delta\epsilon_{ca} = 4.8 \cdot 10^3\ M^{-1} \cdot cm^{-1}$, is in agreement with the estimated value of $\Delta\epsilon = 4.7 \cdot 10^3\ M^{-1} \cdot cm^{-1}$ obtained for the formation of ubisemiquinone [28].

Reaction centers containing menaquinone. In reaction centers containing MQ as the primary quinone, the kinetics at 645 are much different from those containing UQ. The initial slope is nonzero and there is a pronounced shoulder on the kinetic trace during the first illumination (Fig. 5c). This can be qualitatively understood if we assume that the state I^-Q^- is relative long lived (see Appendix, Fig. 10b). A quantitative fit of the theory to the experimental data was obtained by assuming that $k_1 = k_3$ (as was done for UQ) and searching for the best value of k_2. Fig. 5c shows a small deviation between experiment (full line, Fig. 5c) and theory (dotted line). Several factors may contribute to this deviation: incomplete reconstitution with MQ, the neglect of the back reaction of I^- ($t_{1/2} \approx 2$ min) which is approx. 10 times faster than for UQ, the inequivalence of k_1 and k_3, or the inequivalence of $\Delta\epsilon_{ba}$ and $\Delta\epsilon_{dc}$ (Eqn. 16).

The best value for the decay time for I^-MQ^- was determined to be $\tau_2 = 1/k_2 = 5.2 \pm 2$ s (average of four experiments). This time is much slower than in reaction centers containing UQ and helps to stabilize and trap the I^-MQ^- species. It accounts for the observation of the doublet EPR signal in reaction centers containing MQ.

Effect of UQ removal on the kinetics of I^- formation

If, as postulated, the sigmoidal shape of the kinetics is due to a reduction of Q^-, then it should not be observed in reaction centers from which quinone had been removed. This indeed was found, as shown in Fig. 6a, b. The rate of formation of I^- in reaction centers without quinone was 4—5 times faster than the rate in reaction centers containing Q^{2-}. The sigmoidal kinetics were restored when UQ was added back (Fig. 6c). The EPR signal of I^- observed in reaction centers containing no UQ had the same characteristics ($g = 2.0036$, $\Delta H = 13$ G) as that observed in reaction centers containing UQ. In reaction centers that had 1.0 ± 0.1 UQ/reaction center, the kinetic behavior was sigmoidal but showed a nonzero initial slope. This was thought to be due to a fraction (5—10%) of reaction center with no quinone. When excess exogenous quinone was added to saturate all binding sites, the zero slope was restored.

Transient optical absorbance changes due to $I^-(Q^-Fe^{2+})$

The three-step model for the trapping of I^- seems to adequately explain all of the observations discussed so far. Furthermore, the model suggests that the difference in the EPR spectra seen in reaction centers containing UQ and those containing MQ is due to the difference in their decay constant k_2. It was therefore of interest to measure k_2 directly by observing the transient decay of I^-Q^- after a flash of light.

Reaction centers containing UQ. Using a camera flash (0.3 J/cm^2 output energy, $t_{1/2} = 1$msec), a transient absorbance increase ($\lambda = 645$ nm) was observed after the first flash (Fig. 7a). It had a decay time $\tau_2 = 1/k_2 = 10 \pm 1$ ms ($T = 25$°C). Subsequent flashes also illicited absorbance increases. However, the

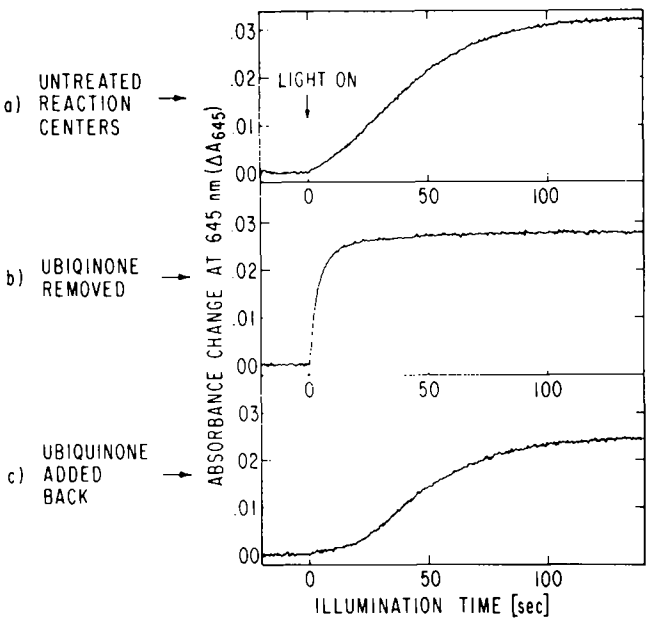

Fig. 6. Effect of removal and readdition of UQ on the kinetics of I^- formation in reaction centers of *R. sphaeroides* during the first illumination. (a) Untreated reaction centers. (b) Reaction centers from which UQ was removed. (c) Reaction centers reconstituted with $2 \cdot 10^{-5}$ M UQ. Reaction center concentrations were approximately 10^{-5} M in 1 mm pathlength cell set at 45° to optical light path. $I = 0.3$ W/cm^2, 2 mM dithionite, 0.2 mM cytochrome *c*, 60 mM Tris-Cl, pH 8. 0.1% Triton X-100, 25°C.

fast decaying component gradually decreased until after ≈20 flashes, only slowly reversible (of the order of minutes) absorbance increases were observed. This is interpreted as being due to the accumulation of the final product I^-Q^{2-}. Reaction centers which had been illuminated continuously and allowed to recover or reaction centers containing no quinone exhibited no transient after the first flash showing only rapid rise in absorbance which was only slowly (of the order of minutes) reversible. Even after the first flash, the fast (10 ms) decay is not completely reversible (Fig. 7a). This may be due to the formation of I^- in reaction centers containing either no Q or Q^{2-} or to the formation of I^-Q^{2-} due to the relatively long flash duration. We believe that the fast (10 ms) component represents the decay of I^-UQ^- (τ_2) and accounts for the lack of a doublet EPR signal in reaction centers containing UQ.

Reaction centers containing MQ. When the flash experiments described above were repeated on reaction centers containing MQ, the decay time for the transient was found to be 4.0 ± 0.5 s, 25°C (see Fig. 7b). This is 400 times longer than observed in reaction centers containing UQ. Again, after subsequent flashes, the fast transient disappeared and was replaced by a slower decay. We believe that the initial transient is the decay of I^-MQ^-.The decay time is in good agreement with that estimated from the kinetics during continuous illumination and is slow enough so that significant amounts of I^-MQ^- may be trapped by illumination while freezing and thus accounts for the observation of the doublet EPR signal in reaction centers containing MQ. The decay times obtained by continuous and pulsed illumination are summarized in Table I.

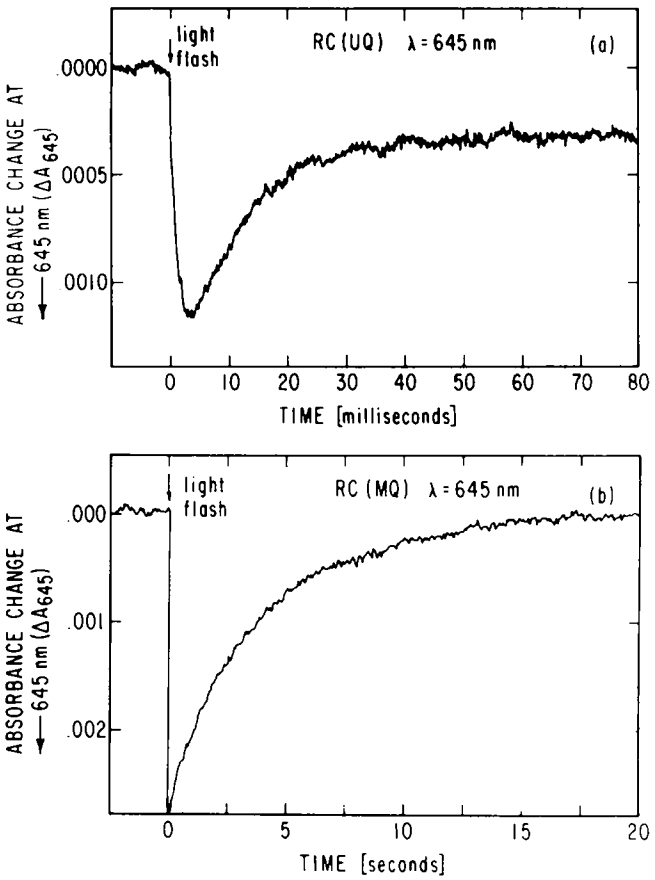

Fig. 7. Transient optical absorbance changes at $\lambda = 645$ nm due to I^-Q^- in reaction centers of *R. sphaeroides* containing UQ (a) and MQ (b), $T = 25^\circ C$. Flash energy = 0.3 J/cm^2, half time = 1 ms, Corning filters CS-2-64, CS-5-56, photodiode UDT 10D blocked with narrow bandpass interference filter and a Bausch and Lomb monochromator. Instrument time constant was 1 ms for (a) and 100 ms for (b). [RC] = $2 \cdot 10^{-6}$ M; 0.2 mM cytochrome *c*, 2 mM dithionite, 60 mM Tris-Cl, pH 8. Samples contained 10^{-5} M UQ-10 (a) and 10^{-5} M vitamin K-1 (b). Note the different time scales in (a) and (b).

TABLE I

DECAY TIMES ($\tau_2 = 1/k_2$) OBTAINED FOR RCs CONTAINING UBIQUINONE AND MENAQUINONE BY CONTINUOUS AND PULSED ILLUMINATION ($I^-Q^- \xrightarrow{k_2} IQ^{2-}$)

Quinone	τ_2 * (sec) continuous illumination	τ_2 ** (sec) pulsed illumination
Ubiquinone	<0.5	0.010 ± 0.001
Menaquinone (Vitamin K-1)	5 ± 2	4.0 ± 0.5

* Obtained from optical kinetics ($\lambda = 645$ nm, $T = 25^\circ C$) using Eqns. 18, 11, and 13, assuming $k_1 = k_3$ (see Fig. 5).

** Obtained from transient decay ($\lambda = 645$ nm, $T = 25^\circ C$) after pulsed illumination. τ_2 is the time it takes to reach 63% (i.e., 100(1 − 1/e)%) of the final value.

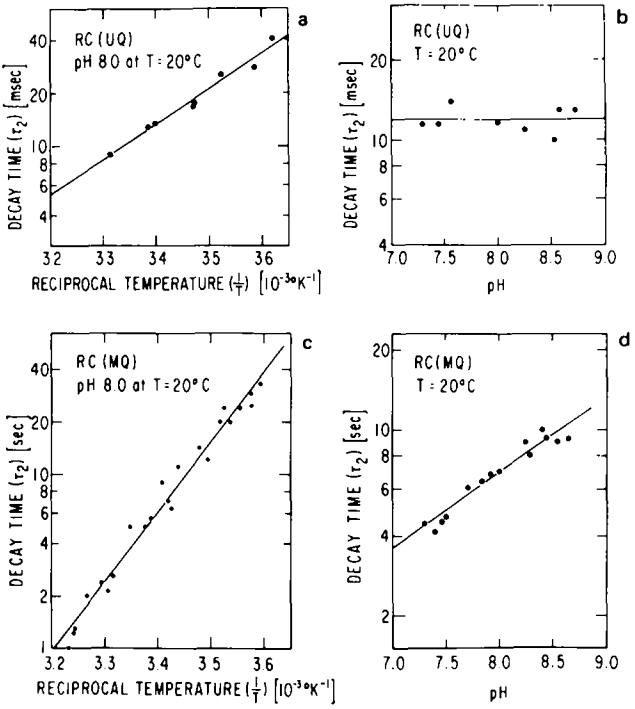

Fig. 8. Dependence of τ_2 on temperature (a, c) and pH (b, d). Flash kinetics were measured on samples, as indicated in the caption for Fig. 7, on reaction centers contraining UQ (a, b) or MQ (c, d). The samples for pH dependence measurements were buffered with Tris (pH 8—9) or HEPES (pH 7—8). The ionic strength was adjusted to be constant (60 mM) with NaCl.

Activation energy

The activation energy of the $I^-Q^- \rightarrow IQ^{2-}$ process was obtained from the temperature dependence of the decay time, τ_2. However, since the pH of the Tris-HCl buffer is temperature dependent [29] and the decay time, in turn is pH dependent, a correction had to be made to account for these dependencies. This was done by assuming, as a first order approximation, that the pH dependence of τ_2 is temperature independent and that the activation energy, $\delta E^{\ddagger}$, is pH independent. We can then write for τ_2 normalized to pH 8 at temperature T

$$\tau_2(T,\ \mathrm{pH}\ 8) = \tau_2^{\mathrm{M}}(T,\ \mathrm{pH})\left[\frac{\tau_2(20^\circ\mathrm{C},\ \mathrm{pH}\ 8)}{\tau_2(20^\circ\mathrm{C},\ \mathrm{pH})}\right] = \tau_0 \exp(\delta E^{\ddagger}/kT \qquad (3)$$

where τ_2^{M} $(T,\ \mathrm{pH})$ is the measured kinetic time at temperature T at the pH of the Tris-Cl buffer at T [29] *. The square bracket represents the pH dependence of τ_2 and was determined experimentally at 20°C (Figs. 8b, d). τ_0 is a constant and k is Boltzmann's constant.

The experimentally determined decay times, τ_2^{M}, are plotted logarithmically against $1/T$ in Figs. 8a and c. From the slope of the lines, the uncorrected

* Typical values of the pH dependence of Tris-Cl are [29]: pH (T = 40°C) = 7.46, pH (T = 20°C) = 8.0, pH (T = 5°C) = 8.46.

activation energies were obtained (Table II). For reaction centers containing UQ, τ_2 was found to be approximately pH independent and no correction was applied. For reaction centers containing MQ, the square bracket of Eqn. 3 was evaluated from the pH dependence as shown in Fig. 9b and the known pH dependence of the buffer. The normalized value of τ_2 (T, pH 8) was replotted logarithmically against $1/T$ and the corrected activation energy was obtained. The results are summarized in Table II.

Kinetics of I^- formation from EPR absorptions

The time dependences of the EPR changes (measured at 2.1 K) were determined by illuminating EPR samples at room temperature for various times

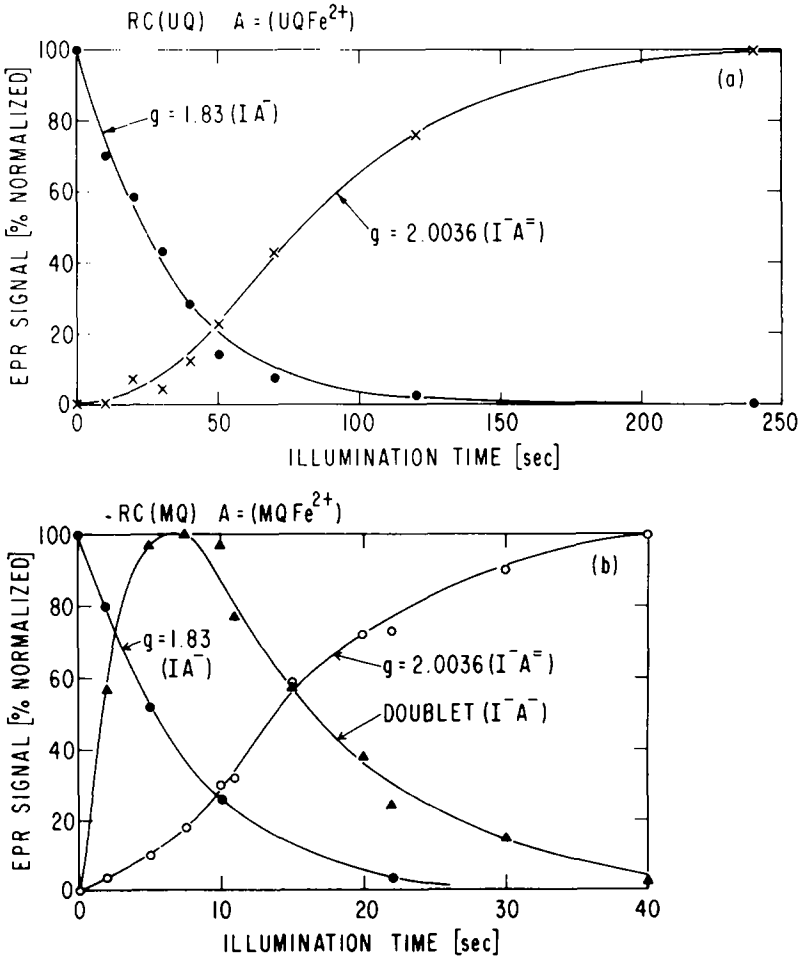

Fig. 9. Kinetics of EPR changes due to I^- formation in reaction centers containing UQ (a) and MQ (b). (a) Amplitudes of EPR signals at $g = 1.83$ (●———●) and $g = 2.0036$, (×———×). $T = 2.1$ K after various illumination periods. ($I = 0.15$ W/cm^2, $T = 25$°C. [RC] = $3 \cdot 10^{-5}$ M, 0.2 mM cytochrome c, 2 mM dithionite, 60 mM Tris-Cl, pH 8. 0.1% Triton X-100.) (b) Amplitudes of EPR signals at $g = 1.8$ (●———●), $g = 2.0036$ (○———○), and the doublet EPR signal (▲———▲) ($T = 2.1$ K) after various illumination periods ($I = 0.4$ W/cm^2, $T = 10$°C) in reaction center samples containing MQ. [RC] = $2 \cdot 10^{-5}$ M, [vitamin K-1] = $2 \cdot 10^{-5}$ M, 0.2% Triton X-100, 0.2 mM cytochrome c, 2 mM dithionite, 60 mM Tris-Cl, pH 8.

TABLE II

ACTIVATION ENERGIES FOR THE ELECTRON TRANSFER FROM I^- TO Q^-Fe^{2+}

Quoted errors are statistical (one standard deviation).

Quinone	$\delta E^{\ddagger}$ (uncorrected) (eV)	$\delta E^{\ddagger}$ (corrected) * (eV)
UQ	0.42 ± 0.03	0.42 ± 0.03 (9.7 kcal/mol)
MQ	0.80 ± 0.03	0.67 ± 0.03 (15.5 kcal/mol)

* Corrected for the pH dependence of the reaction and the temperature dependency of the pH using Eqn. (3).

before freezing. In reaction centers containing UQ, the EPR spectrum of A^- ($g = 1.8$) decreased rapidly with illumination (Fig. 9a) while the EPR spectrum of I^- ($g = 2.0036$) exhibited a lag period similar to that observed in the optical kinetics (Fig. 5a). No doublet signals were observed. When reaction centers, after being illuminated, were kept in the dark for 1 h at room temperature, the I^- signal decayed and the A^- signal did not recover. These results are explained by the three-step model (Eqn. 2) in the following way: (1) The loss of the $g = 1.8$ signal is due to the formation of the diamagnetic $DIQ^2{}^-Fe^{2+}$ state (Eqn. 2). (2) The sigmoidal kinetics of the I^- signal is due to the sequential kinetics. (3) The lack of a doublet EPR signal is due to the rapid decay of $I^-UQ^-Fe^{2+}$. (4) The decay of the I^- signal and lack of recovery of the A^- signal in the dark is due to the decay of $I^-Q^2{}^-Fe^{2+}$ to $IQ^2{}^-Fe^{2+}$. In view of the time required to freeze the EPR samples after illumination and the unknown variation of the rate constants during that period, a quantitative fit of the kinetics of the EPR signal with theory was not attempted.

When reaction centers containing MQ were illuminated, the A^- ($g = 1.8$) signal also decayed exponentially (Fig. 9b) and the I^- ($g = 2.0036$) signal exhibited a lag in its formation (Fig. 9b) similar to that observed in reaction centers containing UQ. In addition, the doublet signal appeared at short illumination times, then decayed away at longer times (Fig. 9b). These results are consistent with the three-step model in which the doublet is due to the intermediate state $I^-(MQ^-Fe^{2+})$ which is stable for a few seconds after formation. The lag in the formation of the narrow I^- signal ($g = 2.0036$) indicates that it is not associated with the same paramagnetic state as the doublet signal. The exponential decay of the A^- ($g = 1.8$) signal (Fig. 9b) is, however, rather surprising; it suggests that in the state $I^-(MQ^-Fe^{2+})$ the EPR spectrum of the ferroquinone (MQ^-Fe^{2+}) complex is appreciably altered due to interaction with I^-. A similar loss of the $g = 1.8$ EPR signal concomitant with doublet formation has also been observed in *R. viridis* [17].

Discussion and Conclusions

The purpose of this study has been to investigate the nature of the intermediate species I^- in reaction centers of *Rps. sphaeroides* R-26 by photoreductive trapping. In particular, we have sought to understand the difference between the EPR properties of I^- in *C. vinosum* chromatophore preparations

where a doublet signal was obtained and those of I^- in reaction centers of *Rps. sphaeroides* R-26 where only a single resonance was observed. We have found that this difference is due to an electron transfer from I^- to Q^-Fe^{2+} whose rate depends on whether the quinone is UQ as in *Rps. sphaeroides* or MQ as in *C. vinosum*. This electron transfer rate can be described by the theories of thermally activated electron tunneling [30,31]. With the aid of these theories, we were also able to estimate the distance between the reactants I^- and MQ^-.

We have constructed a model (Eqn. 2) in which the lack of the doublet signal is due to the decay of the $I^-(UQ^-Fe^{2+})$ state and the appearance of a singlet EPR signal is due to the subsequent formation of $I^-(UQ^{2-}Fe^{2+})$. The proposed model explains the optical and EPR spectra, the sigmoidal kinetics and the effect of UQ removal on the sigmoidal kinetics. The model has been further tested by a quantitative comparison between the experimental data and theoretical kinetic curves. In reaction centers containing UQ the sigmoidal kinetic curves can be fitted well to the experimental data by assuming that the two photoreductive trapping rates k_1 and k_3 are equal, and that the decay of $I^-(UQ^-Fe^{2+})$ proceeds with a rate k_2 that is larger than 2 s^{-1}. An independent measurement of k_2 made by using a short flash showed that k_2 is indeed fast (k_2 = 100 s^{-1}, 25°C) (see Table I).

In order to observe the doublet EPR signal in reaction centers from *Rps. sphaeroides*, the UQ was replaced with menaquinone (vitamin K-1) which had been shown to be the primary quinone in *C. vinosum* [26,27]. The reaction centers containing MQ exhibited different sigmoidal behavior from those containing UQ when subjected to continuous illumination. These kinetics are consistent with a slower decay of $I^-(MQ^-Fe^{2+})$ ($\tau_2 \approx 5 \pm 2$ s, 25°C). An independent measurement of $I^-(MQ^-Fe^{2+})$ by flash illumination gave a transient optical signal due to I^- with a decay time, τ_2 = 4.0 ± 0.5 s (25°C) (see Table I).

The slower decay of $I^-(MQ^-Fe^{2+})$ made it possible to trap the species exhibiting a doublet EPR signal with a splitting (δH = 60 G) identical to that previously reported in *C. vinosum* chromatophores [11—13]. Tiede et al. have proposed that the doublet splitting arises from a magnetic interaction between I^- and Q^-Fe^{2+} [11—13]. Our work supports this proposal and further suggests that the interaction giving rise to the doublet is mainly between I^- and Q^- since the splitting is not present when quinone is reduced to Q^{2-} or when the quinone is absent (i.e. I^- is not split by Fe^{2+} alone). In order to explain the earlier observation of both doublet and singlet EPR signals in *C. vinosum* samples Tiede et al. [13] postulated that the electron on I^- is shared between two molecules, bacteriopheophytin and bacteriochlorophyll, and that the different positions of these two species with respect to Q^-Fe^{2+} gave rise to two EPR signals. Our results suggest a simpler explanation, namely, that those reaction centers which have their quinone doubly reduced (or absent) give rise to the singlet I^- signal, while those which contain Q^-Fe^{2+} give rise to the doublet. The lack of any appreciable broadening of the EPR signal of I^- due to Fe^{2+} is in contrast to the EPR resonances of the reduced primary [20] and secondary [32,33] quinones which are extensively broadened (300 and 450 G, respectively) by the proximity of the paramagnetic Fe^{2+}. These results indicate that Fe^{2+} is closer to Q_1 and Q_2 than it is to I.

The magnetic interaction between I^- and Q^-Fe^{2+} contains information about

the structure and function of the electron transfer complex. There are two contributions to this interaction [34,35,36]. One is due to a magnetic dipole-dipole interaction which varies as the reciprocal third power of the distance between paramagnetic species. The other is due to an exchange interaction which results from the overlap of electronic wavefunctions. The exchange interaction, J, between the reactant molecules I^- and Q^-Fe^{2+} can be related to the tunneling matrix element T_{AB} [37—39] by the expression

$$\frac{J}{2} = -\frac{|T_{AB}|^2}{(E_A - E_B - \Delta)} \tag{4}$$

where E_A and E_B are the redox energies of the donor and acceptor, and Δ is the vibronic coupling parameter. By modifying the theory of thermally induced electron tunneling to include this relation, the following expression for the electron transfer rate k_2 in the high temperature limit was obtained [39]:

$$k_2 = \frac{1}{\tau_2} = \frac{|J|}{2\hbar}\left(\frac{\pi\delta E^\ddagger}{k_B T}\right)^{1/2} \exp -\frac{\delta E^\ddagger}{k_B T} \tag{5}$$

where $\delta E^\ddagger$ is the activation energy and $|J|$ is the exchange coupling, $\hbar$ is Planck's constant/2π, k_B is Boltzmann's constant, T is the absolute temperature. Note that the above expression contains only two parameters, $\delta E^\ddagger$ and $|J|$. These were determined by two independent experiments. Consequently, we were able to use Eqn. 5 to test the applicability of the tunneling mechanism to the electron transfer reaction from I^- to MQ^-Fe^{2+}.

Assuming that the observed doublet splitting is predominantly due to an exchange interaction (to be justified below), the activation energy for this reaction was calculated using Eqn. 5 (τ_2 = 4 s, J = 60 G, T = 298 K) and the result compared with the measured value.

$\delta E^\ddagger$ (experimental) = 0.67 ± 0.03 eV

$\delta E^\ddagger$ (theoretical) = 0.61 eV.

The agreement between these results support the mechanism of thermally activated tunneling for this reaction. For the case where Q = UQ, no doublet was observed, hence we cannot tell whether the tunneling mechanism applies. If we assume that it does, we can use the measured value of τ_2 and $\delta E^\ddagger$ to calculate from Eqn. 5 the ratio of J for UQ and MQ. This ratio is $3.1 \cdot 10^{-2}$, resulting in J (UQ) = 1.8 G.

The large difference (8—10 orders of magnitude) between the electron transfer rate for I^- to Q^-Fe^{2+} and I^- to QFe^{2+} (the physiological case) can be accounted for by the high activation energy for the case in which the primary quinone has to accept two electrons. What is the origin of this unusually high activation energy? In the theory of thermally activated tunneling [30,31], the activation energy arises from the requirement for energy conservation, i.e., the energy loss by the donor has to be equal to the energy gain by the acceptor. This requirement is satisfied only at specific nuclear configurational states of the donor and acceptor molecules which are populated by thermal activation *.

* The lowest of these states is the transition state. For a simple discussion, see Okamura et al. [39].

This leads to an activation energy given by [30,31]:

$$\delta E^{\ddagger} = \frac{(E_A - E_B - \Delta)^2}{4\Delta} \tag{6}$$

where E_A and E_B are the redox energies of the reactants and products and Δ is the vibronic coupling parameter. A large Δ implies a large change in nuclear configuration between reactants $I^-(Q^-Fe^{2+})$ and products $I(Q^{2-}Fe^{2+})$.

The high activation energies for electron transfer from I^- to Q^-Fe^{2+} can thus be reconciled with a large Δ (see Table III). These large Δ values are thought to be due to configurational changes required to accommodate a doubly reduced quinone in an aprotic environment. In contrast, smaller configurational changes (and hence small values of Δ) are expected to be necessary to accomodate a singly reduced quinone. This results in a lower activation energy for the physiological electron transfer from I^- to QFe^{2+}. From Eqn. 6, we see that when Δ just matches the difference in redox energies $E_A \cdot E_B$ (see Table III), a very fast transfer rate is obtained. This matching may be one of the factors involved in optimizing the rate of electron transfer in vivo. The difference in Δ between UQ and MQ is not understood; it may, however, be related to the difference in the pH dependence of τ_2 for UQ and MQ (see Fig. 9b, d). Another effect of the presence of the doubly charged Q^{2-} is approximately a fivefold reduction in the rate of I^- formation as compared to that in reaction centers without quinones (Fig. 6).

The exchange interaction obtained from the doublet spectrum enables one to estimate the distance between I^- and MQ^- (we assume that the interaction is mainly with MQ^- and not Fe^{2+}). Using Eqn. 5 and the values of Δ and $E_A - E_B$ from Table III, we calculate the matrix element to be, $T_{AB} = 10^{-3}$ eV (8 cm^{-1}). Hopfield [30] relates T_{AB} to the distance between nearest neighbor edge atoms, R, by the expression

$$T_{AB} = \frac{2.7}{(N_A N_B)^{1/2}} \exp(-0.72\, R) \tag{7}$$

where N_A, N_B are the number of atoms in the conjugation path of A and B; T_{AB} is a eV and R in Å. Taking these as 18 and 8 for I^- and Q^-, respectively, the distance, R, calculated from Eqn. 7 is 7.5 Å. Jortner [31] used a different relation based on the distance dependence $d(\ln T_{AB})/dR = -1.3$ $Å^{-1}$ with a value of $T_{AB} = 1.24 \cdot 10^{-3}$ eV at $R = 10$ Å. This results in the expression

$$T_{AB} = 5.5 \cdot 10^{+2} \exp(-1.3\, R) \tag{8}$$

With $T_{AB} = 10^{-3}$ eV, this relation gives a distance of 10 Å. For the case of UQ, we had estimated a value of J of 1.8 G, i.e. $T_{AB} = 1.3 \cdot 10^{-4}$ eV (Eqn. 4). Using Eqns. 7 and 8, this results in a distance of 10—12 Å. These distances are in the same range as previous estimates of 9—13 Å obtained by Peters et al. [40] from the kinetics of the $I^-(QFe^{2+}) \rightarrow I(Q^-Fe^{2+})$ reaction.

Having obtained the distance between the paramagnetic molecules I^- and MQ^-, we can calculate the contribution of the magnetic dipole interaction to the doublet spectrum. Since the spin density is delocalized over a molecule whose size is comparable to intermolecular distances the dipolar coupling

TABLE III

PARAMETERS OF THE ELECTRON TRANSFER REACTIONS INVOLVING I^- AND Q^-Fe^{2+}

Reaction	τ(25°C) (s)	$\delta E\ddagger$ (eV)	$E_A - E_B$ (eV)	Δ [e] (eV)	J (Gauss)	T_{AB} (mV)	R (Å)
$I^-MQ^-Fe^{2+} \rightarrow I\,MQ^{2-}Fe^{2+}$	4	0.67	≈0.1 [d]	2.9	60	10^{-3}	7.5—10
$I^-UQ^-Fe^{2+} \rightarrow I\,UQ^{2-}Fe^{2+}$	10^{-2}	0.42	≈0.1 [d]	1.7	1.8 [f]	$1.3 \cdot 10^{-4}$	10—12
$I^-UQ\,Fe^{2+} \rightarrow I\,UQ^-Fe^{2+}$	2×10^{-10} [a]	<0.03 [b]	≈0.5 [c]	≈0.5	—	$(0.6–2.5) \cdot 10^{-4}$ [b]	9—13 [b]

[a] From Rockley et al. [4] and Peters et al. [40].

[b] From data of Peters et al. [40].

[c] Using estimates of E_0' for (BPh/BPh^-) of —0.55 eV [8] and ($UQ\,Fe^{2+}/UQ^-Fe^{2+}$) of —0.05 eV [2].

[d] Estimated values. The values of Δ are not very sensitive to the values assumed for $E_A - E_B$. For example, doubling the value of $E_A - E_B$ changes Δ from 2.9 eV to 3.1 eV for RCs containing MQ.

[e] Obtained from Eqn. 6. There is a second solution giving a very small and unlikely Δ. For a more detailed discussion, see Ref. 39.

[f] Not observed directly. Obtained by using the measured values of τ_2 and $\delta E\ddagger$ to calculate (Eqn. 5) the ratio of J for UQ and MQ.

depends on details of the orientation of the two molecules. Calculations on simple models, using the procedure outlined by Schepler et al. [36], show that the dipolar contribution to the splitting is of the order of 10 G or less, consistent with our assumption that the major source of the observed 60 G splitting is due to an exchange coupling.

This study has characterized in detail the photoreductive trapping reaction in reaction centers of *Rps. sphaeroides*, but has not solved the problem of the definitive chemical identification of the intermediate acceptor I^-. We have shown that I^- is chemically reactive and magnetically coupled with the primary quinone, supporting (but not proving) the accepted idea that it is the transient intermediate acceptor responsible for the charge separation in the state P^f. The optical changes are consistent with bacteriopheophytin but also show some changes characteristic of bacteriochlorophylls. The EPR and ENDOR results are consistent with the possibility that I^- is either a bacteriopheophytin or bacteriochlorophyll anion radical in the monomeric state. The stability and ease of preparation of I^- described in this work should facilitate studies using other techniques (such as resonance Raman scattering or magnetic circular dichroism measurements) to further elucidate the chemical nature of the transient intermediate.

Appendix I

Kinetics of the three-step model

The three-step model can be formulated as a set of consecutive first order irreversible reactions. (Ignoring the slow decay from d → c)

$$a \xrightarrow{k_1} b \xrightarrow{k_2} c \xrightarrow{k_3} d. \tag{9}$$

where a = IQ^-, b = I^-Q^-, c = IQ^{2-}, d = I^-Q^{2-}. The rate equations can be solved to give the time dependent concentrations of all species.

$$[a] = [IQ^-] = a_0 \exp(-k_1 t) \tag{10}$$

$$[b] = [I^-Q^-] = \frac{a_0 k_1}{k_2 - k_1} [\exp(-k_1 t) - \exp(-k_2 t)] \tag{11}$$

$$[c] = [IQ^{2-}] = a_0 k_1 k_2 \left[\frac{\exp(-k_1 t)}{(k_2 - k_1)(k_3 - k_1)} - \frac{\exp(-k_2 t)}{(k_2 - k_1)(k_3 - k_2)} + \frac{\exp(-k_3 t)}{(k_3 - k_2)(k_3 - k_1)} \right] \tag{12}$$

$$[d] = [I^-Q^{2-}] = a_0 \left[1 - \frac{k_2 k_3 \exp(-k_1 t)}{(k_2 - k_1)(k_3 - k_1)} + \frac{k_1 k_3 \exp(-k_2 t)}{(k_2 - k_1)(k_3 - k_2)} - \frac{k_1 k_2 \exp(-k_3 t)}{(k_3 - k_2)(k_3 - k_1)} \right] \tag{13}$$

where a_0 = the initial concentration of species a. Note that although these equations do not hold when any two rate constants are exactly equal, this case

is easily approximated by making them arbitrarily close to each other (e.g. $k_1/k_3 = 1.001$).

The concentrations [a], [b], [c], [d] are monitored optically. We define the differential extinction coefficients:

$$\Delta\epsilon_{da} = \epsilon_d - \epsilon_a = \frac{\Delta A_1}{[RC]} \tag{14}$$

$$\Delta\epsilon_{dc} = \epsilon_d - \epsilon_c = \frac{\Delta A_2}{[RC]} \tag{15}$$

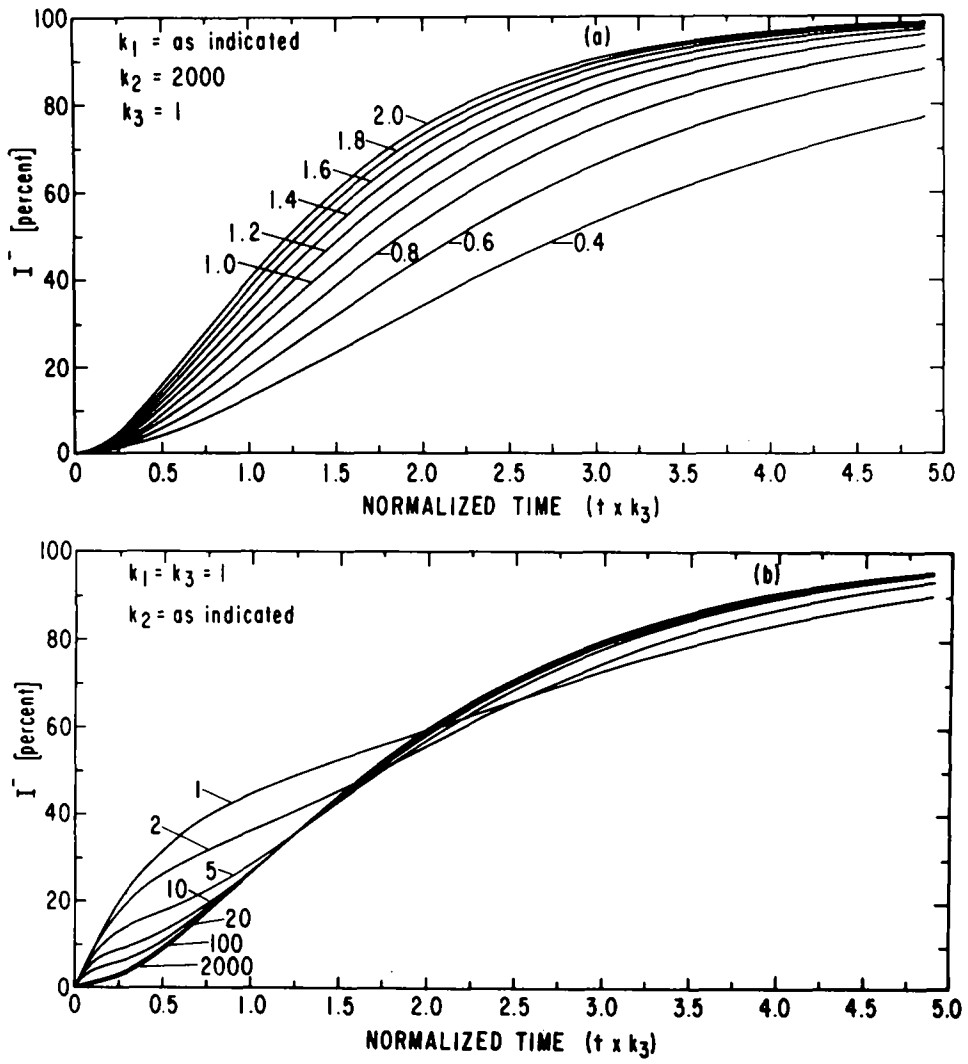

Fig. 10. Theoretical curves describing the changes in the optical absorption due to I^-, using Eqns. 18, 11, and 13 where the absorbance is expressed as per cent I^- ($a_0 = 100$, $\epsilon_{ba} = \epsilon_{da} = 1.0$). The abscissa is the normalized time ($t \times k_3$). (a) The time dependence of I^- for different ratios k_1/k_3 with k_2 large ($k_2 = 2000$). (b) The time dependence of I^- for different values of k_2 with $k_1 = k_3$.

$$\Delta\epsilon_{ba} = \epsilon_b - \epsilon_a = \Delta\epsilon_{dc} \tag{16}$$

$$\Delta\epsilon_{ca} = \epsilon_c - \epsilon_a = \Delta\epsilon_{da} - \Delta\epsilon_{dc} \tag{17}$$

where ΔA_1 and ΔA_2 are the absorbance changes after the first and second illumination, respectively, and [RC] is the reaction center concentration. $\Delta\epsilon_{da}$ and $\Delta\epsilon_{dc}$ are obtained from Eqns. 14 and 15 using the measured values of ΔA_1, ΔA_2, and [RC]. $\Delta\epsilon_{ba}$ and $\Delta\epsilon_{ca}$ are obtained from Eqns. 16 and 17 which assume that the optical changes due to I^- and Q^- are independent of each other.

When the optical absorption changes are monitored at 645 nm, only changes due to I^- (present in species b and d, i.e., $\Delta\epsilon_{ca}^{645} = 0$) are observed and the change in optical absorbance $\Delta A^{645}(t)$ is given by:

$$\Delta A^{645}(t) = \Delta\epsilon_{ba}^{645}[b] + \Delta\epsilon_{da}^{645}[d]. \tag{18}$$

At 645 nm the differential extinction coefficients for forming I^-Q^- from IQ^-, $\Delta\epsilon_{ba}^{646}$, and for forming I^-Q^{2-} from IQ^-, $\Delta\epsilon_{da}^{645}$, are assumed to be equal. Theoretical kinetic curves for several important cases are shown in Fig. 10a; it shows the formation of I^- versus time for different values of k_1 and k_3 for the case $k_2 >> k_1$, k_3. Fig. 10b shows the formation of I^- for different values of k_2 for the case $k_1 = k_3$.

When optical absorption changes are monitored at 450 nm, where UQ^- absorption occurs, the optical absorption change is given by

$$\Delta A^{450}(t) = \Delta\epsilon_{ba}^{450}[b] + \Delta\epsilon_{ca}^{450}[c] + \Delta\epsilon_{da}^{450}[d] \tag{19}$$

where $\Delta\epsilon_{ba}$, $\Delta\epsilon_{ca}$, $\Delta\epsilon_{da}$ are the differential extinction coefficients for forming I^-Q^-, IQ^{2-}, and I^-Q^{2-} from IQ^-. They were obtained from Eqns. 14—17 using the experimentally determined values of A_1, A_2, and [RC].

Acknowledgements

We would like to thank Don Fredkin for clarifying many aspects of the electron tunneling theory, Ed Moskowitz for help in the analysis of the three-step model, and Larry Ackerson and Ed Abresch for technical assistance in preparing reaction centers. This work was supported by grants from the National Science Foundation (PCM 74-21413) and the National Institutes of Health (GM-13191). M.Y.O. acknowledges the support of a PHS Research Career Development Award (GM-00106).

References

1 Feher, G., Okamura, M.Y. (1978) 'Chemical Composition and Properties of Reaction Centers' in The Photosynthetic Bacteria (Clayton, R.K. and Sistrom, W.R., eds.), pp. 349—386, Plenum Press, New York

2 Parson, W.W. and Cogdell, R. (1975) Biochim. Biophys. Acta 416, 105—149

3 Parson, W.W., Clayton, R.K. and Cogdell, R.J. (1975) Biochim. Biophys. Acta 387, 265—278

4 Rockley, M.G., Windsor, M.W., Cogdell, R.J. and Parson, W.W. (1975) Proc. Natl. Acad. Sci. U.S. 72, 2251—2255

5 Kaufmann, K.J., Dutton, P.L., Netzel, T.L., Leigh, J.S. and Rentzepis, P.M. (1975) Science 188, 1301—1304

6 Dutton, P.L., Kaufmann, K.J., Chance, B. and Rentzepis, P.M. (1975) FEBS Lett. 60, 275—280
7 Moskowitz, E. and Malley, M. (1978) Photochem. Photobiol., in the press
8 Fajer, J., Brune, D.C., Davis, M.S., Forman, A. and Spaulding, L.D. (1975) Proc. Natl. Acad. Sci. U.S. 72, 4956—4960
9 Cogdell, R.J., Monger, T.G. and Parson, W.W. (1975) Biochim. Biophys. Acta 408, 189—199
10 Shuvalov, V.A. and Klimov, V.V. (1976) Biochim. Biophys. Acta 440, 587—599
11 Tiede, D.M., Prince, R.C., Reed, G.H. and Dutton, P.L. (1976) FEBS Lett. 65, 301—304
12 Dutton, P.L., Prince, R.C., Tiede, D.M., Petty, K.M., Kaufmann, K.J., Netzel, T.L. and Rentzepis, P.M. (1977) in Brookhaven Symposia in Biology No. 28, pp. 213—237
13 Tiede, D.M., Prince, R.C. and Dutton, P.L. (1976) Biochim. Biophys. Acta 449, 447—467
14 Van Grondelle, R., Romijn, J.C. and Holmes, N.G. (1976) FEBS Lett. 72, 187—192
15 Trosper, T.L., Benson, D.L. and Thornber, J.P. (1977) Biochim. Biophys. Acta 460, 318—330
16 Netzel, T.L., Rentzepis, P.M., Tiede, D.M., Prince, R.C. and Dutton, P.L. (1977) Biochim. Biophys. Acta 460, 467—479
17 Prince, R.C., Tiede, D.M., Thornber, J.P. and Dutton, P.L. (1977) Biochim. Biophys. Acta 462, 467—490
18 Holten, D., Windsor, M.W., Parson, W.W. and Thornber, J.P. (1978) Biochim. Biophys. Acta 501, 112—126
19 Okamura, M.Y., Isaacson, R.A. and Feher, G. (1977) Biophys. J. 17, 149a
20 Okamura, M.Y., Isaacson, R.A. and Feher, G. (1975) Proc. Natl. Acad. Sci. (US) 72, 3491—3495
21 Straley, S.C., Parson, W.W., Mauzerall, D.C. and Clayton, R.K. (1973) Biochim. Biophys. Acta 305, 597—609
22 McElroy, J.D., Mauzerall, D.C. and Feher, G. (1974) Biochim. Biophys. Acta 333, 261—278
23 Feher, G. (1957) Bell Syst. Tech. J. 36, 449—484
24 Fajer, J., Borg, D.C., Forman, A., Dolphin, D. and Felton, R.H. (1973) J. Am. Chem. Soc. 95, 2739—2741
25 Evans, M.C.W., Lord, A.V. and Reeves, S.G. (1974) Biochem. J. 138, 177—183
26 Okamura, M.Y., Ackerson, L.C., Isaacson, R.A., Parson, W.W. and Feher, G. (1976) Biophys. J. 16, 223a
27 Feher, G. and Okamura, M.Y. (1976) Brookhaven Symposia in Biology: No. 28, pp. 183—194
28 Bensasson, R.J. and Land, E.J. (1973) Biochim. Biophys. Acta 325, 175—181
29 Bates, R.G. and Paabo, M. (1976) in Handbook of Biochemistry and Molecular Biology (Fasman, G., ed.), Physical and Chemical Data, Vol. I, Section D, 3rd edn., pp. 353—361, CRC Press, Cleveland, OH
30 Hopfield, J.J. (1974) Proc. Natl. Acad. Sci. U.S. 71, 3640—3644
31 Jortner, J.J. (1976) J. Chem. Phys. 64, 4860—4867
32 Wraight, C.A. (1977) Biochim. Biophys. Acta 459, 525—531
33 Okamura, M.Y., Isaacson, R.A. and Feher, G. (1978) Biophys. J. 21, 8
34 Abragam, A. and Bleaney, B. (1970) in Electron Paramagnetic Resonance of Transition Ions, pp. 491—540, Clarendon Press, Oxford
35 Ruzicka, F.J., Beinert, H., Schepler, K.L., Dunham, W.R. and Sands, R.H. (1975) Proc. Natl. Acad. Sci. U.S. 72, 2886—2890
36 Schepler, K.L., Dunham, W.R., Sands, R.H., Fee, J.A. and Abeles, R.H. (1975) Biochim. Biophys. Acta 397, 510—518
37 Anderson, P.W. (1959) Phys. Rev. 115, 2
38 Hopfield, J.J. (1977) in Electrical Phenomena at the Biological Membrane Level (E. Roux, ed.), Proc. 29th Int. Meeting of the Soc. de Chemie Physique pp. 471—492, Elsevier, Amsterdam
39 Okamura, M.Y., Fredkin, D.R., Isaacson, R.A. and Feher, G. (1979) in Proc. of the Tunneling Conference (Chance, B., et al., eds.), in the press
40 Peters, K., Avouris, P. and Rentzepis, P.M. (1978) Biophys. J. 23, 207—217